Send Orders for Reprints to reprints@benthamscience.ae

The Open Electrical & Electronic Engineering Journal, 2015, *9*, 127-134 127

Open Access

Sneaking Operation Modes in Zero-Current-Switching Converter

Qu Lili[1,*], Zhang Bo[2] and Wallace K.S. Tang[3]

[1]*Department of Automation, Foshan University, Foshan, Guangdong, 528000, P.R. China*

[2]*College of Electric Engineering, South China University of Technology, Guangzhou, 510641, P.R. China*

[3]*Department of Electronic Engineering, City University of Hong Kong, Hong Kong*

Abstract: This paper reports the occurrence of some abnormal operational modes in soft-switching converters. By constructing a Boolean matrix based on the states of the switching components, some unexpected topological states are identified. Consequently, these states excite the abnormal or sneaking operational modes as referred. A three-stage step-up zero-current switching converter is used as an illustrative example and detailed analysis has been carried out. The phenomenon has also been confirmed in experiences, where performance degradation is noticed.

Keywords: Solid-plug conveying, centrifugal extruder, polymer process, mathematics analysis.

1. INTRODUCTION

Pulse-width modulation has been widely employed for the design of switching power supply and motor drives for decades. However, due to the high switching loss in semiconductor, the operational frequency based on hard commutation is limited. This problem has been well addressed by the concept of soft-switching in eighties [1, 2]. Using resonant inductors, capacitors and diode, zero-voltage or zero-current switching is achieved so that switching loss can be greatly reduced. This in turn allows a significant increase of the switching frequency. Some analyses can be referred to [3-5].

There are many concomitant advantages for having a high switching frequency, including higher current regulator bandwidth, smaller reactive component size, and so on. Moreover, the voltage rate of change and the electromagnetic inference are also low in this type of soft-switching power converters (SPC). These distinct advantages have thus greatly enhanced the extensive usage of SPC in industrial and telecommunication applications [3-7].

However, the introduction of resonance components also makes the design and analysis of SPC much more complex (Smith01). Recently, it is also found that unexpected dynamics may be excited in these converters due to the existence of abnormal topological states [8-11]. This is referred as sneaking operational modes (SOMs), which are similar to the sneaking circuits found in electrical and electronic circuits [12].

The occurrence of SOMs is due to several reasons, while the most common one is the deviation of components or the input signal. As illustrated in this paper, for example, a change of load may introduce SOM, even the switching signal remains the same.

The organization of this paper is as follows. In Section 2, a three-stage step-up resonant switched capacitor (RSC) converter is briefly reviewed. It is considered as a typical example of zero-current switching. To reveal the SOMs in the studied RSC, an automated approach based on Boolean matrix is described in Section 3. A detailed dynamical study is then carried out in Section 4. The condition of the occurrence of SOM is mathematically deduced, and it is confirmed both in experiments. Finally, conclusions are drawn in Section 5.

2. A ZERO-CURRENT-SWITCHING CONVERTER

Fig. (**1**) depicts a three-stage step-up resonant switched capacitor (RSC) converter utilizing zero-current switching [14]. The switching devices Q_1 and Q_2 are power MOSFET shunted by its body diode. A resonant inductor L_r is connected in series with the switching capacitors C_{r1} and C_{r2}, forming the resonant unit to create zero-current switching. The duty cycle of operation is designed as 50% while the switches Q_1 and Q_2 are turned ON and OFF alternatively with a period of T_s.

Fig. (**2**) depicts the normal output waveforms of the RSC converter where four operational modes, denoted as Modes I–IV, based on the corresponding topological states, can be identified.

A. Mode I [$t=t_0 \sim t_1$]

Switch Q_2 and diodes D_{a1} and D_{a2} are turned on at t_0 with zero-current. In this mode, C_{r1} and C_{r2} are charged up by the input source V_{in} and the charges stored at C_{b1}, respectively, while the power for the load R_L is supplied by C_{b2}. Eventually, the voltages across C_{r1} and C_{r2}, denoted as v_{Cr1} and v_{Cr2}, reach their maximum values at time t_1.

*Address correspondence to this author at the Department of Automation, Foshan University, Foshan, Guangdong, 528000, P.R. China;
Tel: 13925906648; E-mail: qulili313@163.com

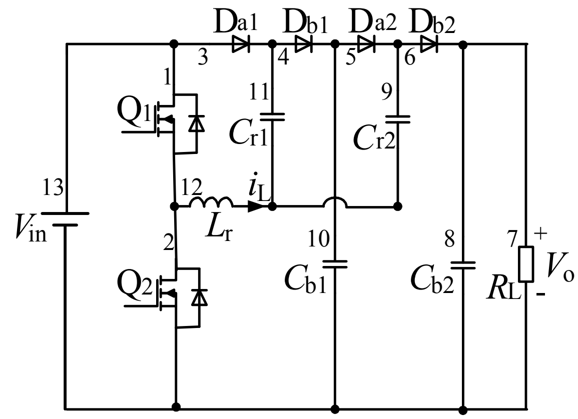

Fig. (1). A three-stage step-up RSC converter.

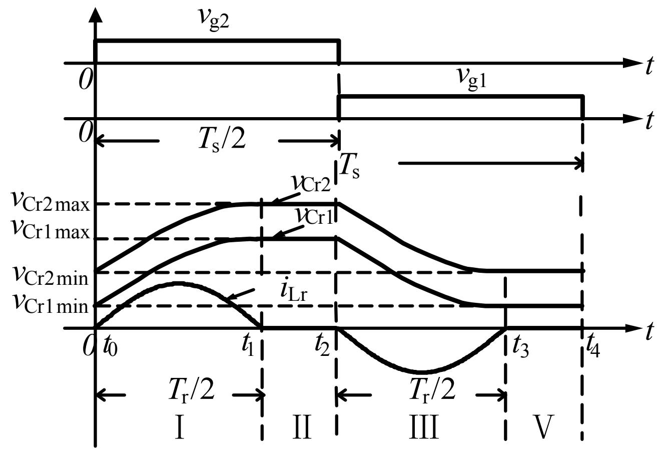

Fig. (2). Waveforms of i_{Lr} and v_{Cr} of the RSC converter.

According to the Kirchhoff's voltage law, we have

$$\begin{cases} V_{in} = v_{Cr1} + v_{Lr} \\ v_{Cb1} = v_{Cr2} + v_{Lr} \end{cases} \tag{1}$$

and the value of v_{Cr1} is governed by

$$v_{Cr1}(t-t_0) = V_{in} - (V_{in} - v_{Cr1}(t_0))\cos(\omega_r(t-t_0)) \tag{2}$$

where $\omega_r = \sqrt{\dfrac{1}{2L_r C_{r1}}}$ is the resonant frequency of L_r and C_r.

From (2) and considering the maximum of v_{Cr1} (denoted as $v_{Cr1\max}$), we have

$$v_{Cr1\max} + v_{Cr1}(t_0) = v_{Cr1}(t_1) - v_{Cr1}(t_0) = 2V_{in} \tag{3}$$

By differentiating (1), it becomes

$$\begin{cases} \dfrac{dV_{in}}{dt} = \dfrac{i_{Cr1}}{C_{r1}} + L_r \dfrac{d^2 i_{Lr}}{dt^2} \\ \dfrac{dv_{Cb1}}{dt} = \dfrac{i_{Cr2}}{C_{r2}} + L_r \dfrac{d^2 i_{Lr}}{dt^2} \end{cases} \tag{4}$$

A very large capacitance is usually employed for the output capacitor C_{b1}. Therefore, v_{Cb1} can be considered as a constant and its derivative is zero. It also implies that the current flowing through C_{r1} and C_{r2} is the same. Hence,

$$i_{Cr1} = i_{Cr2} = \frac{1}{2} i_{Lr} \tag{5}$$

where i_{Cr1} and i_{Cr2} are the currents flowing through C_{r1} and C_{r2}, respectively.

B. Mode II [t_1~t_2]

In Mode II, all the switches Q_i and diodes D_{ai}, D_{bi} are turned off. The voltages v_{Cr1} and v_{Cr2}, are kept unaltered and the capacitor C_{b2} are discharged through R_L, supplying the output power.

C. Mode III [t=t_2~t_3]

In Mode III, the switches Q_1 and diodes D_{b1}, D_{b2} are turn on with zero-current. The output capacitor C_{b1} are charged up by the input voltage V_{in} and the charges stored in C_{r1}. Similarly, C_{b2} is charged up by V_{in} and charges stored in C_{r2}. Both v_{Cr1} and v_{Cr2} become minimal at time t_3.

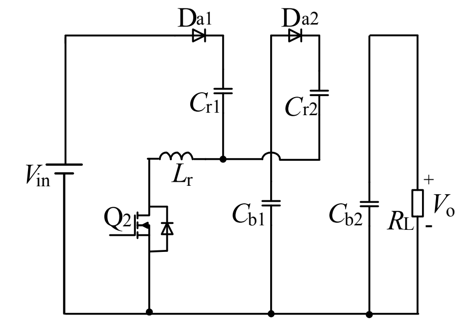

(a) Mode I

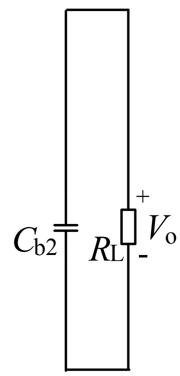

(b) Modes II & IV

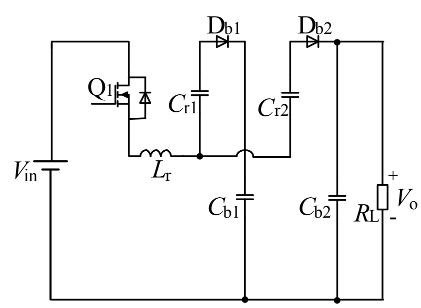

(c) Mode III

Fig. (3). Corresponding circuits of the operational modes for the RSC converter.

D. Mode IV [t=t_3~t_4]

The operation at Mode IV is similar to Mode II, where v_{Cr1} and v_{Cr2} are kept constant at their minimum values.

The associated circuits for the four operational modes are depicted in Fig. (**3**).

For each cycle, the average current flowing to the two switching capacitors should be equal to zero. Denoting $i_{Cr1}^{(1)}$, $i_{Cr1}^{(3)}$ and $i_{Lr}^{(1)}$, $i_{Lr}^{(3)}$ as the current at C_{r1} and L_r in Modes I and III, we have

$$\begin{aligned}&\int_{t_0}^{t_1} i_{Cr1}^{(1)}(t)\,dt+\int_{t_2}^{t_3} i_{Cr1}^{(3)}(t)dt\\&=\frac{1}{2}\int_{t_0}^{t_1} i_{Lr}^{(1)}(t)dt+\int_{t_2}^{t_3} i_{Lr}^{(3)}(t)\,dt=0\end{aligned} \tag{6}$$

Assuming no power loss and equating the input-output power of the circuit, it can also be derived that:

$$\frac{V_{in}}{2}\int_{t_0}^{t_1} i_{Lr}^{(1)}(t)dt-V_{in}\int_{t_2}^{t_3} i_{Lr}^{(3)}(t)\,dt=\frac{V_o}{2}\left[-\int_{t_2}^{t_3} i_{Lr}^{(3)}(t)dt\right] \tag{7}$$

Substitute (6) into (7), we have

$$V_o=3V_{in} \tag{8}$$

It should be remarked that the relationship between the input-output voltages given in (8) is governed by the circuit topology, i.e. the number of stages designed [15].

3. AUTOMATED SNEAK IDENTIFICATION

The circuit analysis in Section 2.1 presents the desired operational modes of the RSC converter given in Fig. (**1**).

Recently, it is found in [9-13] that some sneaking operational modes may exist in power convertor circuits, affecting their performance. In the followings, a scheme for identifying these sneaking operational modes is described.

3.1. Topological States Represented by Boolean Matrix

The on/off stages of switching components, for example the MOSFET and the diodes in Fig. (**1**), govern its operational modes. Referring to Fig. (**1**), the following Boolean matrix can be constructed:

$$A=\begin{bmatrix} 0&0&0&0&0&0&1&1&1&1&1&1&1\\ 0&0&0&0&0&1&1&1&1&1&1&1&1\\ 0&0&0&0&1&0&1&1&1&1&1&1&1\\ 0&0&0&0&1&1&1&1&1&1&1&1&1\\ 0&0&0&1&0&0&1&1&1&1&1&1&1\\ 0&0&0&1&0&1&1&1&1&1&1&1&1\\ \cdot&\cdot&\cdot&\cdot&\cdot&\cdot&\cdot&\cdot&\cdot&\cdot&\cdot&\cdot&\cdot\\ 1&1&1&0&1&0&1&1&1&1&1&1&1\\ 1&1&1&0&1&1&1&1&1&1&1&1&1\\ 1&1&1&1&0&0&1&1&1&1&1&1&1\\ 1&1&1&1&0&1&1&1&1&1&1&1&1\\ 1&1&1&1&1&0&1&1&1&1&1&1&1\\ 1&1&1&1&1&1&1&1&1&1&1&1&1 \end{bmatrix} \tag{9}$$

where

1. each column represents the on/off state of a component in the design; the 1st to 6th columns represent the MOSFETs Q_1, Q_2 and Diodes D_{a1}, D_{b1}, D_{a2}, D_{b2} while the 7th to 13th columns represent $R_L, C_{b2}, C_{r2}, C_{b1}, C_{r1}, L_r$ and V_{in} as indicated in Fig. (**1**);
2. the state of a switching component can be '1' and '0' denoting the state of 'on' and 'off', respectively;
3. the state of a non-switching components, e.g. capacitors, inductors or resistors, is always '1' (Note: these columns are dummy and can be deleted. They are only included for completeness).
4. each row represents a potential circuit of the power converter

It is obvious that the possible number of states is 2^n where n is the number of switching components in the circuit. However, many of them are in fact invalid and the matrix A in (9) can be reduced to its simplest form.

3.2. Qualitative Reasoning and Knowledge

In order to extract the sneaking operational modes, it is required to eliminate all the invalid topologies represented by (9). It can be achieved based on qualitative reasoning and the circuit theory. Referring to the RSC in Fig. (**1**), the following principles of operations are established:

1. Since the duty cycle of the main switches, Q_1 and Q_2, is 50% and they are not allowed to be on or off at the same time, any row with same symbol in the first two column (i.e. . state of Q_1 = state of Q_2) should be eliminated. Particularly, all the switches Q_i and diodes D_{ai}, D_{bi} are turned off which represent Mode II and IV in Fig. (**3**) should be reserved.
2. To achieve zero-current switching, the circuit must involve both capacitor and inductor. Therefore, using Figs. (**1 and 9**) as an example, it is an invalid circuit if the following pairs of diodes are both turned on: (D_{a1}, D_{b1}), (D_{b1}, D_{a2}), (D_{a2}, D_{b2}) or (D_{a1}, D_{b2}).
3. Uni-directional switching devices, i.e. diode in our circuit, with reversed direction cannot be turned on.
4. To obtain the simplest Boolean matrix, a sub-string is considered as a dummy, which can always be deleted. The definition of a sub-string is given in Definition 1.

Definition 1: Let $p=\{p_i\}$ and $q=\{q_i\}$ are two rows in the Boolean matrix, q is a sub-string of p if $q_i \le p_i, \forall i$.

3.3. Sneaking Mode Identification

Based on the description given in Section 3.2, a MATLAB program has been developed to automatically generate the simplest Boolean Matrix and create the circuits. Equation (10) shows the final simplest matrix B obtained:

$$B=\begin{bmatrix} 0&0&0&0&0&0&1&1&1&1&1&1&1\\ 0&1&0&1&0&1&1&1&1&1&1&1&1\\ 0&1&1&0&1&0&1&1&1&1&1&1&1\\ 1&0&0&1&0&1&1&1&1&1&1&1&1\\ 1&0&1&0&1&0&1&1&1&1&1&1&1 \end{bmatrix} \tag{10}$$

As compared with the normal operational modes given in Fig. (**3**), which can be represented by the following matrix B_0:

$$B_0=\begin{bmatrix} 0&0&0&0&0&0&1&1&1&1&1&1&1\\ 0&1&1&0&1&0&1&1&1&1&1&1&1\\ 1&0&0&1&0&1&1&1&1&1&1&1&1 \end{bmatrix} \tag{11}$$

It can be concluded that two sneaking operational modes exist which are represented by the matrix C.

$$C=\begin{bmatrix} 0&1&0&1&0&1&1&1&1&1&1&1&1\\ 1&0&1&0&1&0&1&1&1&1&1&1&1 \end{bmatrix} \tag{12}$$

The corresponding circuits are also automatically generated in MATLAB program as depicted in Fig. (**4**).

4. DYNAMICAL ANALYSIS AND OBSERVATIONS

4.1. Analysis of the Sneaking Operation Mode

To further justify the existence of the sneaking operational modes (Modes I' and III') in the studied RSC, a detailed circuit analysis is performed.

Referring to the Mode I' given in Fig. (**4a**), the inductance current will not go to zero after the normal Mode I. Instead, it will be kept excited in the branches, C_{r1}-D_{b1}-C_{b1}-D_{Q2}-L_r and C_{r2}-D_{b2}-C_{b2}-D_{Q2}-L_r. Define $i_{Cr1}^{(1')}$ as the current flowing through C_{r1}, it is derived that

$$i_{Cr1}^{(1')}(t)=\frac{v_{Cb1}-v_{Cr1\max}}{2Z_r}\sin\big(\omega_r(t-t_1)\big) \tag{13}$$

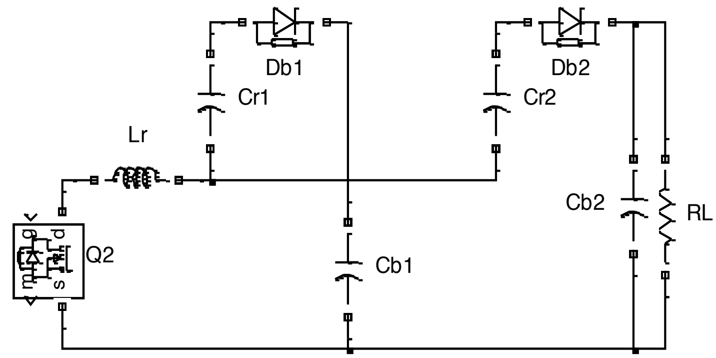

(a) Mode I'

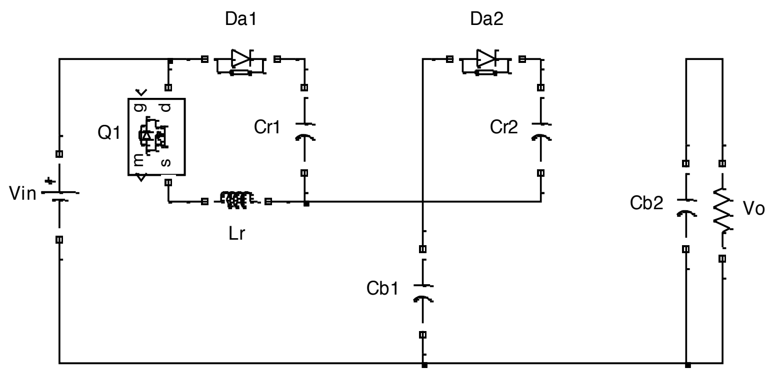

(b) Mode III'

Fig. (4). Corresponding topologies for the sneaking operational modes

where $\omega_r = \sqrt{\dfrac{1}{2L_r C_{r1}}}$ and $Z_r = \sqrt{\dfrac{L_r}{2C_{r1}}}$.

Similarly, as indicated in the Mode III' shown in Fig. (**4b**), the inductance current will continuously be excited after the normal Mode III via the branches D_{a1}-C_{r1}-L_r-D_{Q1} and C_{b1}-D_{a2}-C_{r2}-L_r-D_{Q1}-V_i. Denoting $i_{Cr1}^{(3')}$ as the current flowing through C_{r1} in Mode III', it can be obtained that

$$i_{Cr1}^{(3')}(t) = \frac{-v_{Cr1\min}}{2Z_r}\sin(\omega_r(t-t_4)) \tag{14}$$

where the voltage at switching capacitor C_{r1} is

$$v_{Cr1}(t-t_4)v_{Cr1\min}\cos(\omega_r(t-t_4)) \tag{15}$$

with

$$v_{Cr1}(t_0) = v_{Cr1}(t_5) = -v_{Cr1\min} \tag{16}$$

Similar to the normal modes, it can also be proved that the currents flowing through the switching capacitors are the same, and hence the relationship (5) holds.

In Modes I' and III', the output power at the load is given as:

$$\frac{-V_o}{2}\int_{t_1}^{t_2} i_{Lr}^{(1')}(t)dt + \int_{t_3}^{t_4} i_{Lr}^{(3')}(t)\,dt = \frac{V_o^2}{R_L}T_s \tag{17}$$

where $i_{Lr}^{(1')}$ and $i_{Lr}^{(3')}$ represent the inductance current in Modes I' and III', respectively, T_s is the period of one cycle.

Consider the capacitor voltage v_{Cr1} during t_1~t_4, the voltage difference is

$$\begin{aligned} & v_{Cr1\max} - v_{Cr1\min} \\ & = -\frac{1}{C_r}\left[\int_{t_1}^{t_2} i_{Cr1}^{(1')}(t)dt + \int_{t_3}^{t_4} i_{Cr1}^{(3')}(t)\,dt\right] \\ & = -\frac{1}{2C_r}\left[\int_{t_1}^{t_2} i_{Lr}^{(1')}(t)dt + \int_{t_3}^{t_4} i_{Lr}^{(3')}(t)\,dt\right] \end{aligned} \tag{18}$$

Substitute (17) into (18),

$$v_{Cr1\max} - v_{Cr1\min} = \frac{V_o}{R_L C_r f_s} \tag{19}$$

where $f_s = \dfrac{1}{T_s}$.

However, from (3) and (16), it is given that

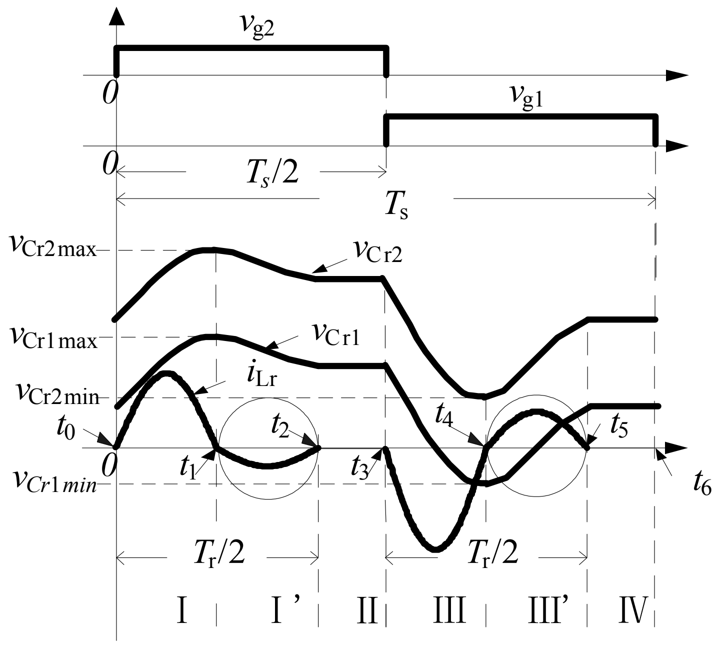

Fig. (5). Waveforms of the RSC converter with sneaking operational modes. (f_r>2f_s).

$$v_{Cr1\max} - v_{Cr1\min} = 2V_{in} \tag{20}$$

By comparing (19) and (20), we have

$$\frac{V_o}{V_{in}} = 2R_L C_r f_s \tag{21}$$

As shown in (21), the input-output ratio is no longer a constant when sneaking operation modes occur. The resultant output waveforms are depicted in Fig. (**5**). Since the input-output ratio is linearly proportional to $R_L C_r f_s$, the output voltage and power will be reduced, causing the deterioration of the output characteristics.

4.2. Condition of Existence

As shown in Fig. (**5**), the currents $i_{Lr}^{(1')}$ and $i_{Lr}^{(3')}$ in Modes I' and III' are non-zero. From (13) and (14), the conditions for the occurrence of sneaking operational modes can be obtained as:

$$\begin{cases} v_{Cb1} - v_{Cr1\max} < 0 \\ v_{Cr1\min} < 0 \end{cases} \tag{22}$$

When t=t_0,

$$v_{Lr}(t_0) = V_{in} - v_{Cr1}(t_0) = v_{Cb1} - v_{Cr2}(t_0) \tag{23}$$

and when t=t_1,

$$v_{Lr}(t_1) = v_{Cb1} - v_{Cr1}(t_1) = v_{Cb2} - v_{Cr2}(t_1) \tag{24}$$

Since

$$v_{Cr1}(t_1) - v_{Cr1}(t_0) = v_{Cr2}(t_1) - v_{Cr2}(t_0) = \frac{1}{2C_r}\int_{t_0}^{t_1} i_{Lr}^{(1')}(t)\,dt \tag{25}$$

From (23)-(25), we have

$$\Delta V = V_{in} - v_{Cb1} = v_{Cb1} - v_{Cb2} = V_o - v_{Cb1} \tag{26}$$

and

$$\Delta V = \frac{V_o - V_{in}}{2} \tag{27}$$

Therefore,

$$v_{Cb1} = V_{in} + \Delta V = V_{in} + \frac{V_o - V_{in}}{2} \tag{28}$$

Substitute (28) into (22), the occurrence condition for the sneaking operational modes is

$$R_L C_r f_s < 1.5 \tag{29}$$

4.3. Experimental Results

In order to experimentally confirm the analysis given in the previous sections, the RSC converter in Fig. (**1**) has been built with the components listed in Table **1**.

To operate in its normal operational modes, $R_L C_r f_s > \frac{3}{2}$. An example is given in Fig. (**6a**) where V_{in}=2V, f_s=42kH and $R_L = 22\Omega > \frac{1.5}{C_r f_s} = 17.8\Omega$. However, when the load drops below the critical value, sneaking operational modes are excited and the resultant output waveforms are obtained as depicted in Fig. (**6b**). It clearly shows that the results are well matched with the analytical ones. Minor deviation is noticed which is probably due to the internal resistance of power supply and the forward voltage drops in the diodes.

Table 1. Components for the realization of RSC converter.

	Symbols in Fig. (1)	**Device or Values**
MOSFET Switches	$Q_{1,2}$	IRFZ44N
Schottky Diodes	$D_{1,2,3,4}$	S30SC4M
Resonant inductor	L_r	320nH
Switching capacitors	$C_{r1,r2}$	2mF
Output capacitors	$C_{b1,b2}$	330mF

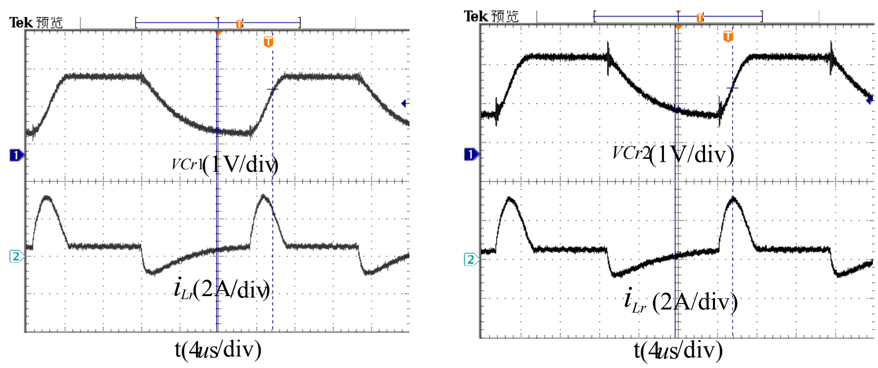

(a) Normal operational modes with R_L=22Ω

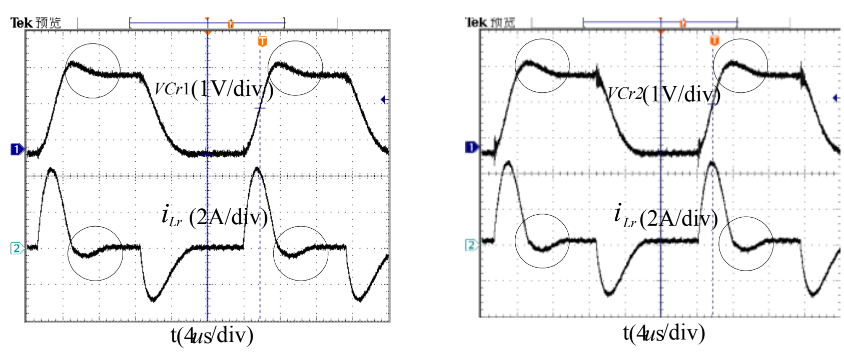

(b) Sneaking operational modes with R_L=8.9Ω

Fig. (6). Output waveforms obtained in experiment for different loads.

CONCLUSION

In this paper, the existence of sneaking operational modes in soft-switching power converter is reported. They are excited by some undesired topological states, which can be revealed by the construction of a Boolean matrix, representing all the feasible on-off states of the switching components. In particular, a common 3-stage step-up resonant switched capacitor converter has been analyzed. It is mathematically proved that, if certain condition is fulfilled, sneaking operational modes will occur and the dynamics of the power converter are affected. This phenomenon is also confirmed both in simulations and experiments. Finally, it should be remarked that similar analysis can be performed in the designs of other power converters or soft-switching devices, serving as a performance and reliability test.

CONFLICT OF INTEREST

The author confirms that this article content has no conflict of interest.

ACKNOWLEDGEMENTS

This work was financially supported by National Natural Science Foundation of China (51277030) and Foundation for

High-level Talents in Higher Education of Guangdong Provincial (2050205-194).

REFERENCES

[1] K. H. Liu, and F. C. Lee, "Resonant switches-a unified approach to improve performances of switching converters," In: *Proc. IEEE Int. Telecommunications Energy Conf.*, pp. 334-341, 1984.

[2] K. H. Liu, and F. C. Lee, "Zero-voltage switching technique in DC/DC converters," *IEEE Trans. Power Electron*, vol. 5, no. 3, pp. 293-304, 1990.

[3] M. C. Caponet, F. Profumo, and A. Tenconi, "Evaluation of power losses in power electronic converters for industrial applications: Comparison among hard switching, ZVS and ZVS-ZCS converters," In: *Proc. Power Conversion Conf.*, vol. 3, pp. 1073-1077, 2002.

[4] P. Das, and G. Moschopoulos, "A comparative study of zero-current transition PWM converters," *IEEE Trans. Indust Electron*, vol. 54, no. 3, pp. 1319-1328, Jun. 2007.

[5] K. M. Smith, and K. M. Smedley, "Engineering design of lossless passive soft switching methods for PWM converter I: With minimum voltage stress circuit cells," *IEEE Trans. Power Electron*, vol.16, no.3, pp.336-344, 2001.

[6] Y. C. Chuang, and Y. L. Ke, "High-efficiency and low-stress ZVT–PWM DC-to-DC converter for battery charger," *IEEE Trans. Indust Electron*, vol.55, no.8, pp.3030-3037, 2008.

[7] M. G. Egan, D. L. O'Sullivan, J. G. Hayes, M. J. Willers, and C. P. Henze, "Power-factor-corrected single-stage inductive charger for electric vehicle batteries," *IEEE Trans. Industrial Electronics*, vol. 54, no. 2, pp. 1217-1226, 2007.

[8] Y. M. Liu, and L. K. Chang, "Single-stage soft-switching AC–DC converter with input-current shaping for universal line applications," *IEEE Trans. Indust. Electron*, vol. 56, no. 2, pp. 467-479, 2009.

[9] J. Li, D. Qiu, and B. Zhang, "Sneak circuit analysis for n-stage resonant switched capacitor converters based on graph theory," in *Proc. IEEE Annual Conf. Industrial Electronics Society*, pp. 1581-1585, Nov. 2007.

[10] D. Qiu, and B. Zhang, "Discovery of sneak circuit phenomena in resonant switched capacitor DC-DC converters," In: *Proc. IEEE Conf. Industrial Electronics and Applications*, pp.1-4, May 2006.

[11] W. Tu, D. Qiu, B. Zhang, and J. Li, "Sneak circuit analysis in n-stage resonant switched capacitor converters," In: *Proc. IEEE Int. Workshop Anti-counterfeiting*, *Security, Identification*, pp.61-65, 2007.

[12] C. J. Price and N. Hughes, "Effective automated sneak circuit analysis," In: *Proc. Annual Symp. Reliability and Maintainability*, pp. 356-360, Jan 2002.

[13] W. Tu, D. Qiu, B. Zhang, and J. Li, "General laws of sneak circuit in resonant switched capacitor converters," In: *Proc. IEEE Power Electronics Specialists Conf.*, pp.708-712, 2007.

[14] K. K. Law, K. W. E. Cheng, and Y. P. B. Yeung, "Design and analysis of switched-capacitor-based step-up resonant converters," *IEEE Trans. Circ. Syst.-I*, vol. 52, no. 5, pp. 943-948, 2005.

[15] C. Zhao, X. Wu, P. Meng, and Z. Qian, "Optimum design consideration and implementation of a novel synchronous rectified soft-switched phase-shift full-bridge converter for low-output-voltage high-output-current applications," *IEEE Trans. Power Electron*, vol.24, no.2, pp.388-397, 2009.

Received: December 15, 2014 Revised: January 04, 2015 Accepted: February 25, 2015